

STATISTICAL ANALYSIS PLAN (SAP)

In vivo differentiation of basal cell carcinoma subtypes by microvascular and structural imaging using Dynamic optical coherence tomography

Version: 1.0 (March 22, 2017)

Collaborators/authors:

Lotte Themstrup¹, Nathalie De Cavalho², Sabrina Mai Nielsen³, Jonas Olsen¹, Silvana Ciardo², Sandra Schuh⁴, Birgit Meinecke-Hansen Nørnberg⁵, Julia Welzel⁴, Martina Ulrich⁶, Giovanni Pellacani², Gregor B. E. Jemec¹

1: Department of Dermatology, Zealand University Hospital, Roskilde, Denmark

2: Department of Dermatology, University of Modena and Reggio Emilia, Modena, Italy

3: Musculoskeletal Statistics Unit, The Parker Institute, Bispebjerg and Frederiksberg Hospital, Frederiksberg, Copenhagen, Denmark.

4: Department of Dermatology and Allergology, General Hospital Augsburg, Augsburg, Germany

5: Department of Pathology, Zealand University Hospital, Roskilde, Denmark

6: CMB/Collegium Medicum Berlin, Berlin, Germany

Statistical Analyst

Sabrina M. Nielsen, BSc, MSc; Research fellow

Musculoskeletal Statistics Unit, The Parker Institute, Bispebjerg and Frederiksberg Hospital, Frederiksberg, Copenhagen, Denmark.

Statistical Advisor

Robin Christensen, Senior Biostatistician, MSc, PhD

Professor of Clinical Epidemiology, adj*

Head of Musculoskeletal Statistics Unit (MSU),

The Parker Institute, Bispebjerg and Frederiksberg Hospital,

Nordre Fasanvej 57

DK-2000 Copenhagen F

Denmark

Study synopsis

The study is a cross-sectional study designed to identify key microvascular and structural features of basal cell carcinoma (BCC) using in vivo Dynamic optical coherence tomography (OCT) imaging and to explore whether these features can be used for non-invasive subtyping of BCC lesions.

Superficial BCC, nodular BCC, and infiltrative BCC are three common types of BCC and investigating microvascular and structural features using Dynamic optical coherence tomography (OCT) for distinguishing these has not been done before.

In this study, 81 patients with a total of 98 BCC lesions (55 nBCC, 27 sBCC, 16 iBCC) from three European clinical dermatology centres (ROS, MOD, AUG) underwent Dynamic optical coherence tomography of their BCC lesions.

Study Objectives

The objective of this study was to identify key microvascular and structural features of basal cell carcinoma (BCC) using in vivo Dynamic optical coherence tomography (OCT) imaging and to explore whether these features can be used for non-invasive subtyping of BCC lesions.

Hypotheses

Dynamic-OCT:

- a) "Circumscribed vessels" are present more often in nodular BCC (nBCC) than in superficial BCC (sBCC) and infiltrative BCC (iBCC).
This feature is most likely found at depth 300µm and 500µm
- b) "Flare" is present more often in sBCC than in nBCC and iBCC.
This feature is most likely found at depth 150µm and 500µm
("Flare" is defined as a smudge-red vascular appearance¹)
- c) Branching/arborizing vessels:
 - i) Branching/arborizing vessels are present more often in nBCC and iBCC than in sBCC
 - ii) Branching/arborizing vessels are **more** strongly present (+++) in nBCC and in iBCC compared to sBCC.
 - iii) Branching/arborizing vessels are **less** strongly present (+++) in sBCC compared to nBCC and iBCC
The arborizing/branching feature is most likely found at depth 300µm and 500µm
- d) The pattern "Chaos" is present more often in iBCC than in sBCC and nBCC
This feature is most likely found at depth 300µm and 500µm.

Structural OCT:

- a) "Demarcated, hyporeflective ovoid structures" are present more often in nBCC than in sBCC + iBCC.
- b) The size of "Demarcated, ovoid structures" is larger in nBCC than in sBCC and iBCC
- c) "Hyporeflective structures protruding from epidermis" is present more often in sBCC than in nBCC and iBCC.
- d) "Dark peripheral border" is present more often in sBCC than in nBCC and iBCC²
- e) "Arelective cystic structures" is present more often in nBCC and iBCC than in sBCC
- f) "Focal thinning of epidermis" is present more often in nBCC than in iBCC and sBCC

- g) "Fine hyperreflective lines between nests" is present more often in iBCC than in nBCC and sBCC³
- h) The combination of "Demarkated, hyporeflexive ovoid structures" and "Focal thinning of epidermis" is present more often in nBCC than in iBCC and sBCC
- i) The combination of "Hyporeflexive structures protruding from epidermis" and "Dark peripheral border" is present more often in sBCC than in iBCC and nBCC²

Combination of dynamic-OCT and structural OCT:

- a) When "Circumscribed vessels" are present "Demarkated, hyporeflexive ovoid structures" are also present. Both are expected to be present more often in nBCC than in iBCC and sBCC.
- b) When "Branching" is present, "Demarkated, hyporeflexive ovoid structures" are also present. Both are expected to be present more often in nBCC and iBCC than in sBCC.
- c) When "Thinning of epidermis" is present, "Demarkated, hyporeflexive ovoid structures" are also present. Both are expected to be present more often in nBCC than in iBCC and sBCC.
- d) When "Flare" is present, "Hyporeflexive structures protruding from epidermis" are also present. Both are expected to be present more often in sBCC than in iBCC and nBCC.

METHODS

Study design and setting

Patients with primary BCC lesions referred for treatment at one of the three European clinical dermatology centres (ROS, MOD, AUG) and scanned with D-OCT from 21st of August 2014 to 31th of October 2016, were included in the study. Lesions were excluded if the pathology report did not include information about the histopathological subtype. The institutional review board from each centre approved the study (SJ-408) and all patients provided written informed consent in accordance with the principles of the Declaration of Helsinki. Patients were aged > 18 years and all BCC lesions were imaged with D-OCT prior to treatment.

The inclusion of patients resulted in 81 patients with 98 BCC lesions (subtypes: 55 nBCC, 27 sBCC, 16 iBCC), out of 118 patients with 146 BCC lesions (i.e. 37 patients with 48 lesions were excluded because of missing subtype in the pathology report).

Measurements and evaluations

The patients' BCC lesions were histopathologically subtyped from specimens acquired by either punch biopsy (2 or 3 mm), curettage biopsy, or surgical excision.

Dynamic OCT – image acquisition

All of the D-OCT images were acquired using a commercially available multi-beam, Fourier domain OCT scanner (VivoSight Dx, Michelson Diagnostics, Kent, UK) with a centre wavelength of 1305 nm, an in vivo optical resolution of $< 7.5\mu\text{m}$ lateral; $< 5\mu\text{m}$ axial, an A-Line rate of 20 kHz (swept-source laser) and a scan area (field of view) of 6x6 mm. The in vivo imaging depth of the VivoSight OCT scanner is around 1-1.5 mm (tissue dependent) for structural OCT images of the skin and a minimum depth of 500 μm for microcirculation images of the skin. The D-OCT images are presented in a cross-sectional (vertical) and an en-face (horizontal) view. The microcirculation data is acquired simultaneously with the structural OCT grey-scale data and displayed as an overlay in red colour. The technical specifications behind acquiring in vivo D-OCT images of the microcirculation has previously been described⁴. Each BCC lesion was OCT scanned using a multi-slice modality creating a 'stack' of 120 B-scans (in the x-y plane) in order to form a 3D image block. A full scan takes 30 seconds and was acquired without the use of a coupling medium. The skin surface was not prepared prior to scanning and the images were obtained by placing the hand-held probe directly on the skin using a fitted plastic spacer for stability and carefully avoiding compression of the skin. The D-OCT scans were collected by experienced D-OCT users.

Dynamic OCT – analysis of the microvasculature images

In order to evaluate the vascular features in the D-OCT images we applied the terminology and guidelines described in the manuscript "Dynamic optical coherence tomography of skin blood vessels - terminology and practical guidelines" (submitted manuscript) some of which include identifying prominent vascular shapes and evaluating the D-OCT images at three predefined skin depths of 150, 300 and 500 μm . In order to view the D-OCT images at fixed depths beneath the skin surface we utilized software (Michelson Diagnostics, Kent, UK and University of Modena and Reggio Emilia, Modena, Italy) that detects the skin surface and allows the imaged skin area (36 mm^2) to be viewed at the desired depth below the skin surface regardless of skin roughness, as described in previous publications^{5,6}. In short, the software detects the skin surface and allows the imaged skin area (36 mm^2) to be viewed at the desired depth below the skin surface regardless of skin roughness. This 'Fitted en-face' maneuver is performed as post processing and it takes a maximum of ten seconds to process each 3D image block (120 B-scans) using the build-in feature (VivoSight Dx, Michelson Diagnostics, Kent, UK).

For the purpose of this study, 'Fitted en-face' D-OCT still-images from the three predefined image depths (150, 300 and 500 μm) were prepared and randomized, creating a D-OCT en-face

study set of 294 images. Two of the authors (LT, NDC) performed blinded evaluations of the randomized study set assessing:

- a) The presence of each vascular shape (dots, blobs, coils, lines, curves, serpiginous)
- b) The presence of specific vascular characteristics (arborizing vessels, vessels creating a circumscribed figure, vascular flare)
- c) The vascular pattern (no pattern, mottle, mesh, cloud, chaos).

The presence of each vascular shape was rated on an ordinal scale: 0) not present (= presence of <3 vessels of the specific shape), 1) slightly present (+ = presence of ≥ 3 and <10 vessels of the specific shape), 2) highly present (+++ = presence of ≥ 10 vessels of the specific shape). Also, the number of arborizing vessels was scaled: 0) no arborizing vessels, 1) slightly present (+ = presence of ≥ 1 and <5 arborizing vessels) 2) highly present (++ ≥ 5 arborizing vessels).

The observers were blinded to histopathological subtype; clinical appearance and location of the BCC lesions.

Blinded quantitative measurements of the diameter of the largest vascular diameter in the D-OCT en-face images were acquired at each predefined depth (150, 300, 500 μm) using an image processing tool (ImageJ; available from NIH, imagej.nih.gov/ij/). One observer (LT) performed all of the quantitative measurements.

Structural OCT – analysis of structural images

For each BCC lesion, cross-sectional structural OCT scans (full image ‘stacks’ of 120 OCT images) were exported in standard TIFF format creating a study set of 98 structural OCT scans. Two observers (JO and LT) performed blinded evaluations of each entire structural OCT image stack using ImageJ (available from NIH, imagej.nih.gov/ij/). In order to evaluate the structural features in the cross-sectional OCT images we used selected criteria in keeping with OCT features previously described in studies of OCT of BCC²³⁷⁸. The included structural OCT criteria were:

- a) Sharply demarcated hyporeflective ovoid structures located within the dermis
- b) Hyporeflective ovoid structures protruding from epidermis/dermoepidermal junction (DEJ)
- c) Dark peripheral border at the margin of hyporeflective ovoid structures
- d) Areflective cystic areas
- e) Focal thinning of epidermis in relation to hyporeflective structures
- f) Fine hyperreflective lines between adjacent nests.

Furthermore, the size of the hyporeflective structures (A) and (B) were estimated as primarily small; ii) primarily large; iii) primarily mixed.

The observers were blinded to histopathological subtype; clinical appearance and location of the BCC lesions.

STATISTICAL METHODS

Characteristics of patients and lesions

The characteristics of the patients and lesions will be described presenting continuous outcomes as means with corresponding standard deviations (SD), ordinal outcomes (or continuous data that are not normally distributed) as medians with corresponding interquartile range (IQR), and binary outcomes as numbers with corresponding percentages.

Primary analysis

The primary analyses will be based on mixed effects logistic regression models investigating if there is an association with the type of BCC and microvascular features or structural features. The outcome will be coded as present (given the value 1) or non-present of a specific BCC type (given the value 0), and the model will be repeated for each of the three BCC types. Hence, the presence of microvascular and structural features in one specific BCC type will be compared with the presence in the two other BCC types.

The model will be adjusted for all available factors that are expected to influence the result (hypothesis driven model). No correction for multiple testing will be done. All models will be tested for their assumptions. The function `glmer()` from the package `lme4`⁹ will be used in the statistical program R (version 3.3.3)¹⁰.

For the analyses of microvascular features:

BCC type = [feature] + biopsy technique + location + depth + age + gender + (lesion) + (patient) + (pathologist) + (centre)

All variables, except age will be treated as categorical variables. Lesion, patient, pathologist, and centre (lesion nested within patient, which is nested within pathologist, which is nested within centre) are random factors, [feature] is the different types of microvascular features of BCC, and BCC type is a binary variable.

For the analyses of structural features:

BCC type = [feature] + biopsy technique+ location + age + gender + (patient) + (pathologist) + (centre)

All variables, except age will be treated as categorical variables. Patient, centre and pathologist (nested within centre) are random factors, [feature] is the different types of structural features of BCC, and BCC type is a binary variable.

The program code for the primary in the statistical program R:

```
library(lme4)

#For the analyses of microvascular features:
m <- glmer(DiagnosisA ~ Feature1 + BiopsyTechnique + Location + Depth + Age +
Gender + (1 | Center/Pathologist/PtId/LesionID), data = d, family = binomial)
s <-summary(m);s
exp(s$coefficients[,1])

#For the analyses of structural features:
m <- glmer(DiagnosisA ~ Feature1 + BiopsyTechnique + Location + Age + Gender + (1
| Center/Pathologist/PtId), data = d, family = binomial)
s <-summary(m);s
exp(s$coefficients[,1])
```

Secondary analyses

- Exploratory analysis using multiple correspondence analysis (MCA) will be used for investigate the relationships between the different microvascular and structural features. The analysis will be conducted using the function MCA() from the package FactoMinerR¹¹ in the statistical program R (version 3.3.3). There will be conducted three analyses – one for each of the depths (150, 300, and 500 µm).

The following variables will be included in the analysis:

Dots (present, not present)
Blobs (present, not present)
Coils (present, not present)
Lines (present, not present)
Curves (present, not present)
Serpiginous (present, not present)
Arborizing vessels (present, not present)
Vessels creating a circumscribed figure (present, not present)
Vascular flare (present, not present)
The vascular pattern (No pattern, Mottle, Mesh, Cloud, Chaos)
Sharply demarcated hyporeflective ovoid structures located within the dermis (present, not present)
Hyporeflective ovoid structures protruding from epidermis/DEJ (present, not present)
Dark peripheral border at the margin of hyporeflective ovoid structures (present, not present)
Areflective cystic areas (present, not present)
Focal thinning of epidermis in relation to hyporeflective structures (present, not present)
Fine hyperreflective lines between adjacent nests (present, not present)

Sensitivity analysis

- Stratified analyses of microvascular features according to depth, i.e. including only data from the depth of 150, 300, and 500 μm , respectively. It is expected that a depth of 300 μm provides the best circumstances for interpreting the images for some of the features (deeper may result in too much noise and less deep may result in too few visible vessels).
- Univariate models (**BCC type = [feature] + (lesion) + (patient) + (pathologist) + (centre)**, where lesion, patient, pathologist, and centre (lesion nested within patient, which is nested within pathologist, which is nested within centre) are random factors).
- Data-driven models adjusted for all variables (i.e. lesion characteristics, microvascular and structural features, where depth is only an option for the analyses of microvascular features) proven to be significant from univariate analysis (**BCC type = [feature] + [significant variables] + (lesion) + (patient) + (pathologist) + (centre)**, with the exception of those based on the same variable (i.e. present and degree of presence). Lesion, patient, pathologist, and centre (lesion nested within patient, which is nested within pathologist, which is nested within centre) are random factors).

Anticipated tables of the study report

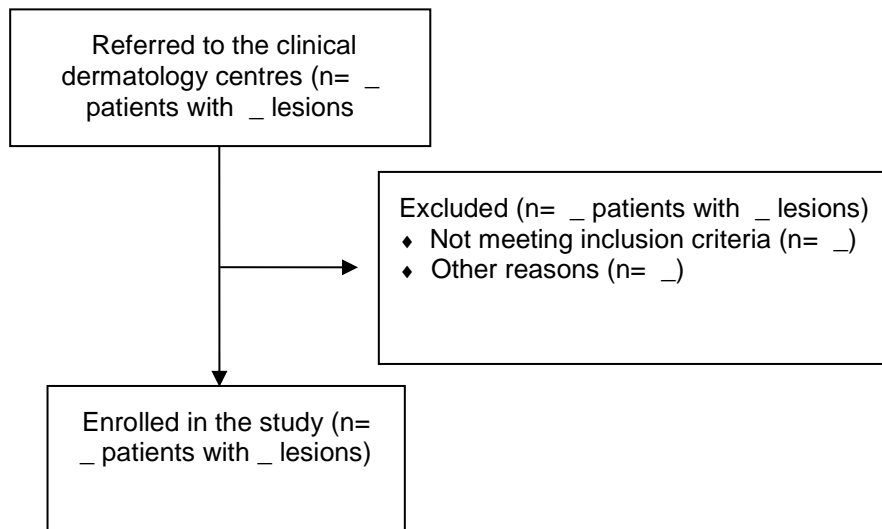


Figure 1: Flow diagram

Table 1: Patient characteristics

Variable	(n =)
Gender, n females (%)	
Age, mean (SD)	
Number of lesions	
1, n (%)	
2, n (%)	
3, n (%)	
4, n (%)	
Diagnosis	
sBCC, n (%)	
nBCC, n (%)	
iBCC, n (%)	
Combined, n (%)	
Centre	
ROS, n (%)	
MOD, n (%)	
AUG, n (%)	

BCC, basal cell carcinoma; iBCC, infiltrative BCC; nBCC, nodular BCC; n, number; SD, standard deviation; sBCC; superficial BCC.

Table 2: Lesion characteristics and frequency of microvascular and structural features of BCC

	Superficial BCC (n =)	Nodular BCC (n =)	Infiltrative BCC (n =)
Lesion characteristics			
Location			
Sun exposed (scalp, face, nose, ear, neck), n (%)			
Relatively sun unexposed (trunk, extremities), n (%)			
Biopsy technique			
Punch biopsy (2 or 3 mm), n (%)			
Curettage biopsy, n (%)			
Surgical excision, n (%)			
Microvascular features (numbers only presented at 300 µm)†			
Dots (0-2), median (IQR)			
Dots			
0: Not present (<3 vessels of this shape), n (%)			
1: Slightly present (≥3 to <10 vessels), n (%)			
2: Highly present (≥10 vessels), n (%)			
Blobs (0-2), median (IQR)			
Blobs			
0: Not present (<3 vessels of this shape), n (%)			
1: Slightly present (≥3 to <10 vessels), n (%)			
2: Highly present (≥10 vessels), n (%)			
Coils (0-2), median (IQR)			
Coils			
0: Not present (<3 vessels of this shape), n (%)			
1: Slightly present (≥3 to <10 vessels), n (%)			
2: Highly present (≥10 vessels), n (%)			
Lines (0-2), median (IQR)			
Lines			
0: Not present (<3 vessels of this shape), n (%)			
1: Slightly present (≥3 to <10 vessels), n (%)			
2: Highly present (≥10 vessels), n (%)			
Curves (0-2), median (IQR)			
Curves			
0: Not present (<3 vessels of this shape), n (%)			
1: Slightly present (≥3 to <10 vessels), n (%)			
2: Highly present (≥10 vessels), n (%)			
Serpiginous (0-2), median (IQR)			
Serpiginous			
0: Not present (<3 vessels of this shape), n (%)			
1: Slightly present (≥3 to <10 vessels), n (%)			
2: Highly present (≥10 vessels), n (%)			
Arborizing vessels (0-2), median (IQR)			
Arborizing vessels			
0: None, n (%)			
1: Slightly present (≥1 to <5 arborizing vessels), n (%)			
2: Highly present (≥5 arborizing vessels), n (%)			
Vessels creating a circumscribed figure, n (%)			
Vascular flare, n (%)			
The vascular pattern			
No pattern, n (%)			
Mottle, n (%)			
Mesh, n (%)			
Cloud, n (%)			
Chaos, n (%)			
Structural features‡			
Sharply demarcated hyporeflective ovoid structures located within the dermis			
0: Not present, n (%)			
1: Primarily small, n (%)			
2: Primarily mixed, n (%)			
3: Primarily large, n (%)			
Hyporeflective ovoid structures protruding from epidermis/DEJ			
0: Not present, n (%)			
1: Primarily small, n (%)			
2: Primarily mixed, n (%)			
3: Primarily large, n (%)			
Dark peripheral border at the margin of hyporeflective ovoid structures, n (%)			
Arefective cystic areas, n (%)			
Focal thinning of epidermis in relation to hyporeflective structures, n (%)			
Fine hyperreflective lines between adjacent nests, n (%)			

BCC, basal cell carcinoma; DEJ, dermoepidermal junction; iBCC, infiltrative BCC; IQR, Interquartile range; nBCC, nodular BCC; n, number;

sBCC; superficial BCC.

Table 3: Association between the type of BCC and microvascular features or structural features of BCC

	Superficial BCC OR (95%CI)	Nodular BCC OR (95%CI)	Infiltrative BCC OR (95%CI)
Microvascular features†			
Dots present <i>Degree of presence</i> 0: Not present (<3 vessels of this shape) 1: Slightly present (≥3 to <10 vessels) 2: Highly present (≥10 vessels)	[Reference level]	[Reference level]	[Reference level]
Blobs present <i>Degree of presence</i> 0: Not present (<3 vessels of this shape) 1: Slightly present (≥3 to <10 vessels) 2: Highly present (≥10 vessels)	[Reference level]	[Reference level]	[Reference level]
Coils present <i>Coils degree of presence</i> 0: Not present (<3 vessels of this shape) 1: Slightly present (≥3 to <10 vessels) 2: Highly present (≥10 vessels)	[Reference level]	[Reference level]	[Reference level]
Lines present <i>Degree of presence</i> 0: Not present (<3 vessels of this shape) 1: Slightly present (≥3 to <10 vessels) 2: Highly present (≥10 vessels)	[Reference level]	[Reference level]	[Reference level]
Curves present <i>Degree of presence</i> 0: Not present (<3 vessels of this shape) 1: Slightly present (≥3 to <10 vessels) 2: Highly present (≥10 vessels)	[Reference level]	[Reference level]	[Reference level]
Serpiginous present <i>Degree of presence</i> 0: Not present (<3 vessels of this shape) 1: Slightly present (≥3 to <10 vessels) 2: Highly present (≥10 vessels)	[Reference level]	[Reference level]	[Reference level]
Arborizing vessels present <i>Degree of presence</i> 0: None 1: Slightly present (≥1 to <5 arborizing vessels) 2: Highly present (≥5 arborizing vessels)	[Reference level]	[Reference level]	[Reference level]
Vessels creating a circumscribed figure			
Vascular flare			
The vascular pattern No pattern Mottle Mesh Cloud Chaos	[Reference level]	[Reference level]	[Reference level]
Structural features‡			
Sharply demarcated hyporeflective ovoid structures located within the dermis <i>Degree of presence</i> 0: Not present 1: Primarily small 2: Primarily mixed 3: Primarily large	[Reference level]	[Reference level]	[Reference level]
Hyporeflective ovoid structures protruding from epidermis/DEJ <i>Degree of presence</i> 0: Not present 1: Primarily small 2: Primarily mixed 3: Primarily large	[Reference level]	[Reference level]	[Reference level]
Dark peripheral border at the margin of hyporeflective ovoid structures			
Areflective cystic areas			
Focal thinning of epidermis in relation to hyporeflective structures			
Fine hyperreflective lines between adjacent nests			

95%CI, 95% confidence interval; BCC, basal cell carcinoma; DEJ, dermoepidermal junction; iBCC, infiltrative BCC; nBCC, nodular BCC; n, number; OR, odds ratio; sBCC; superficial BCC.

* Significant.

†Mixed effects logistic regression adjusted for biopsy technique, location, depth, age, gender, lesion, patient, pathologist, and centre, where lesion, patient, pathologist, and centre (lesion nested within patient, which is nested within pathologist, which is nested within centre) are random factors.

‡ Mixed effects logistic regression adjusted for biopsy technique, location, age, gender, patient, pathologist, and centre, where patient, centre and pathologist (nested within centre) are random factors.

[Plot(s) from MCA analysis]

Figure 2a-c: Plots from explorative analysis of the relationships between the microvascular and structural features using MCA analysis, at the depths 150, 300, and 500 µm.

Appendix Table X: Association between the type of BCC and microvascular features of BCC at the **depth of 150µm**

	Superficial BCC OR (95%CI)	Nodular BCC OR (95%CI)	Infiltrative BCC OR (95%CI)
Microvascular features†			
Dots present			
<i>Degree of presence</i>			
Not present (<3 vessels of this shape)	[Reference level]	[Reference level]	[Reference level]
Slightly present (≥3 to <10 vessels)			
...

95%CI, 95% confidence interval; BCC, basal cell carcinoma; DEJ, dermoepidermal junction; iBCC, infiltrative BCC; nBCC, nodular BCC; n, number; OR, odds ratio; sBCC; superficial BCC.

* Significant.

†Mixed effects logistic regression adjusted for biopsy technique, location, depth, age, gender, lesion, patient, pathologist, and centre, where lesion, patient, pathologist, and centre (lesion nested within patient, which is nested within pathologist, which is nested within centre) are random factors.

Appendix Table X: Association between the type of BCC and microvascular features of BCC at the **depth of 300µm**

	Superficial BCC OR (95%CI)	Nodular BCC OR (95%CI)	Infiltrative BCC OR (95%CI)
Microvascular features†			
Dots present			
<i>Degree of presence</i>			
Not present (<3 vessels of this shape)	[Reference level]	[Reference level]	[Reference level]
Slightly present (≥3 to <10 vessels)			
...

95%CI, 95% confidence interval; BCC, basal cell carcinoma; DEJ, dermoepidermal junction; iBCC, infiltrative BCC; nBCC, nodular BCC; n, number; OR, odds ratio; sBCC; superficial BCC.

* Significant.

†Mixed effects logistic regression adjusted for biopsy technique, location, depth, age, gender, lesion, patient, pathologist, and centre, where lesion, patient, pathologist, and centre (lesion nested within patient, which is nested within pathologist, which is nested within centre) are random factors.

Appendix Table X: Association between the type of BCC and microvascular features of BCC at the **depth of 500µm**

	Superficial BCC OR (95%CI)	Nodular BCC OR (95%CI)	Infiltrative BCC OR (95%CI)
Microvascular features†			
Dots present			
<i>Degree of presence</i>			
Not present (<3 vessels of this shape)	[Reference level]	[Reference level]	[Reference level]
Slightly present (≥3 to <10 vessels)			
...

95%CI, 95% confidence interval; BCC, basal cell carcinoma; DEJ, dermoepidermal junction; iBCC, infiltrative BCC; nBCC, nodular BCC; n, number; OR, odds ratio; sBCC; superficial BCC.

* Significant.

†Mixed effects logistic regression adjusted for biopsy technique, location, depth, age, gender, lesion, patient, pathologist, and centre, where lesion, patient, pathologist, and centre (lesion nested within patient, which is nested within pathologist, which is nested within centre) are random factors.

Appendix Table X: Association between the type of BCC and lesion characteristics, microvascular features or structural features of BCC using **univariate models**

	Superficial BCC OR (95%CI)	Nodular BCC OR (95%CI)	Infiltrative BCC OR (95%CI)
Lesion characteristics‡			
Location			
Sun exposed (scalp, face, nose, ear, neck)	[Reference level]	[Reference level]	[Reference level]
Relatively sun unexposed (trunk, extremities)			
Biopsy technique			
Punch biopsy (2 or 3 mm)	[Reference level]	[Reference level]	[Reference level]
Curettage biopsy			
Surgical excision			
Microvascular features†			
Dots present			
<i>Degree of presence</i>			
Not present (<3 vessels of this shape)	[Reference level]	[Reference level]	[Reference level]
Slightly present (≥3 to <10 vessels)			
...

* Significant.

†Univariate models adjusted only for random factors, i.e. lesion, patient, pathologist, and centre (lesion nested within patient, which is nested within pathologist, which is nested within centre).

‡ Univariate models adjusted only for random factors, i.e. patient, pathologist, and centre (patient nested within pathologist, which is nested within centre).

Appendix Table X: Association between the type of BCC and microvascular features or structural features of BCC using **multivariate data-driven models**

	Superficial BCC OR (95%CI)	Nodular BCC OR (95%CI)	Infiltrative BCC OR (95%CI)
Microvascular features			
Dots present			
<i>Degree of presence</i>			
Not present (<3 vessels of this shape)	[Reference level]	[Reference level]	[Reference level]
Slightly present (≥3 to <10 vessels)			
...

* Significant.

†Mixed effects logistic regression adjusted for significant variables from the univariate analysis, in addition to random factors, i.e. lesion, patient, pathologist, and centre (lesion nested within patient, which is nested within pathologist, which is nested within centre).

‡ Mixed effects logistic regression adjusted for significant variables from the univariate analysis, in addition to random factors, i.e. patient, pathologist, and centre (patient nested within pathologist, which is nested within centre).

References

1. Tehrani H, McArthur P, Dalal M. Visualizing the vascular history of nonmelanoma skin tumors: an in vivo human study. *Annals of plastic surgery* 2013;**70**(6):717-9.
2. Cheng HM, Lo S, Scolyer R, et al. Accuracy of optical coherence tomography for the diagnosis of superficial basal cell carcinoma: a prospective, consecutive, cohort study of 168 cases. *The British journal of dermatology* 2016;**175**(6):1290-300.
3. Meekings A, Utz S, Ulrich M, et al. Differentiation of Basal Cell Carcinoma Subtypes in Multi-Beam Swept Source Optical Coherence Tomography (MSS-OCT). *Journal of drugs in dermatology : JDD* 2016;**15**(5):545-50.
4. Ulrich M, Themstrup L, de Carvalho N, et al. Dynamic Optical Coherence Tomography in Dermatology. *Dermatology* 2016;**232**(3):298-311.
5. Themstrup L, Ciardo S, Manfredi M, et al. In vivo, micro-morphological vascular changes induced by topical brimonidine studied by Dynamic optical coherence tomography. *J Eur Acad Dermatol Venereol* 2016;**30**(6):974-9.
6. Manfredi M, Grana C, Pellacani G. Skin Surface Reconstruction and 3D Vessels Segmentation in Speckle Variance Optical Coherence Tomography. *Proceedings of the 11th Joint Conference on Computer Vision, Imaging and Computer Graphics Theory and Applications* 2016;**4**.
7. Hussain AA, Themstrup L, Jemec GB. Optical coherence tomography in the diagnosis of basal cell carcinoma. *Arch Dermatol Res* 2015;**307**(1):1-10.

8. Coleman AJ, Richardson TJ, Orchard G, et al. Histological correlates of optical coherence tomography in non-melanoma skin cancer. *Skin Res Technol* 2013;**19**(1):10-9.
9. Bates D, Maechler M, Bolker B, et al. Fitting Linear Mixed-Effects Models Using lme4. *Journal of Statistical Software* 2015;**67**(1):1-48.
10. R_Core_Team. R: A language and environment for statistical computing. Secondary R: A language and environment for statistical computing. 2017. <https://www.R-project.org/>.
11. Le S, Josse J, Husson F. FactoMineR: An R Package for Multivariate Analysis. *Journal of Statistical Software* 2008;**25**(1):1-18.